

## VISCOSITY OF POLYMERIC LIQUIDS THROUGH MONTECARLO SIMULATIONS

### Objectives

After completing the reading of this chapter, you will be able to:

Define shear modulus and relaxation modulus of a fluid.

Calculate viscosity from relaxation modulus.

Use the Lennard-Jones potential in a multiple chain system.

Devise a Monte Carlo simulation program to calculate relaxation modulus.

Match experimental viscosity data with the viscosity data obtained through MC simulations.

Visualize the configurations of a few polymer blends.

### Keywords

Relaxation modulus, Viscosity, Polymer blend, Lennard-Jones potential, Langevin dynamics.

### **Introduction**

In the earlier chapter you have learnt how the Monte Carlo (MC) simulations can be exploited to investigate motion of a single polymer chain. In this chapter, MC simulations are extended to multiple chain systems and the simulation data have been used to calculate viscosities of a series of polymeric liquids. These are then matched with the experimental viscosity data.

Dynamic viscosities of a series of blends of poly(ethylene glycol) (PEG) and poly(ethylene glycol-*ran*-propylene glycol) (PEG-*ran*-PPG) were measured at a temperature above the melting point. The viscosity data could be fitted into an analytical function involving the volume fraction of PEG,  $\phi_{\text{PEG}}$ . Through coarse-grained MC simulations, stress relaxation curves for each of the pure components and the nine blend compositions of PEG and PEG-*ran*-PPG were obtained. Integration of the stress relaxation modulus gives the viscosity of the sample. The calculated viscosity data through simulation could also be fitted into an analytical function in terms of  $\phi_{\text{PEG}}$ , similar to the one obtained for the experimental viscosity data. A typical stress relaxation curve exhibits two distinct relaxation modes, *viz.* a fast mode having its origin from the energetic-interactions-driven motion of the bond-segments, and a slow mode which originates from the entropy-driven motions of the whole polymer chain. One can fit a stretched exponential function to the fast mode relaxation while a Rouse stress relaxation prescription is an appropriate description of the slow mode relaxation. The intermediate time region of the stress relaxation can also be fitted into three different power functions in time.

## Polyethylene glycol (PEG) and Polypropylene glycol (PPG)

Polyethylene glycol (PEG) is an industrially important polyether compound (used in cosmetics, food and pharmaceuticals, water-based coatings, lubricants, dye carriers for paints, anti-static agents in textile manufacture and oral healthcare products) which often finds clinical applications. PEG is synonymous to polyethylene oxide (PEO) and polyoxyethylene (POE). Usually PEG refers to oligomers and polymers with molar mass less than 20,000 g/mol while PEO refers to polymers of molar mass more than 20,000 g/mol. On the other hand, POE is not characterized by any specific molar mass range. Although PEG and PEO with different molecular weights find use in different applications and have different physical properties (like viscosity) due to chain length effects, their chemical properties are nearly identical. PEG or PEO has the following structure,  $\text{HOCH}_2\text{-(CH}_2\text{-O-CH}_2\text{)}_n\text{CH}_2\text{OH}$ .

Polypropylene glycol (PPG) is the homo-polymer of propylene glycol,  $\text{CH}_3\text{-CHOH-CH}_2\text{OH}$ . PPG usually refers to the polymers of low to medium range molar mass polymer, with the end group as a hydroxyl group. Using the PEG and PPG as precursors, often random polymers are prepared such as poly(ethylene glycol-*ran*-propylene glycol) ( $\equiv$  PEG-*ran*-PPG), which finds its use as a quenchant, lubricant and foam control agent and also as a surfactant. The PEG-*ran*-PPG has the structure  $\text{H-(O-CH}_2\text{-CH}_2\text{)}_x\text{(O-CH(CH}_3\text{)-CH}_2\text{)}_y\text{(O-CH}_2\text{-CH}_2\text{)}_z\text{OH}$ . The polymer is a liquid at room temperature facilitating its suitability to be used as a surfactant in various applications.

In this chapter, we intend to look into the bulk rheological properties of the PEG:PEG-*ran*-PPG system, since overall viscosity of the blend has a deterministic role in the formation and stability of the resulting film on drying. For this purpose, we have measured the dynamic viscosity of several blends at the mixing temperature of 150°C. In order to supplement the measured dynamic viscosities of the blend compositions, we have performed coarse-grained Monte Carlo simulations on these systems. Viscosity values have been obtained by integrating the calculated stress relaxation modulus  $G(t)$  function for each of the blend systems as well as of the pure components. The results show that there is a one-to-one correspondence between the measured and simulated bulk viscosities.

### Viscosity measurements on PEG, PEG-*ran*-PPG and their blends

The samples of PEG (MW 10,000 g/mol) and PEG-*ran*-PPG (MW 12,000 g/mol) were purchased from Sigma Aldrich. [Sigma Aldrich Product Catalogue ([www.sigmaaldrich.com](http://www.sigmaaldrich.com)) 2010. **Poly(ethylene glycol)**: Fluka Product No 81280; Molwt 10,000; Vapor pressure < 0.01 mm Hg (20°C); Auto-ignition temperature 305°C; Melting range 62-65°C. **Poly(ethylene glycol-*ran*-propylene glycol)**: Aldrich Product No 438200; Average  $M_n \sim 12,000$ ; Density 1.092 g/mL (25°C); Refractive index  $n_{20/D}$  1.466; Viscosity 35,000 cSt (25°C); Boiling point > 200°C; Pour point 4°C.]

The blend compositions were prepared by melt-mixing the pre-weighed components at  $150 \pm 5$  °C. We had prepared nine blend compositions corresponding to PEG volume fraction ( $\phi_{\text{PEG}}$ ) 0.1,

0.2, 0.3, 0.4, 0.5, 0.6, 0.7, 0.8 and 0.9. The dynamic viscosities of the nine blend samples and also of the individual components (PEG and PEG-*ran*-PPG) were measured with the help of a Brookfield viscometer (Brookfield Dial Reading Viscometer, Model LVT, Brookfield Engineering Laboratories Inc., USA), at a temperature of  $150 \pm 5$  °C. We have used the LV1 spindle at the lowest speed of 0.3 rpm. The decision for the working temperature for viscosity measurements was prompted by the determination of cloud point temperatures of the blends. For this purpose, the blends were prepared at  $150 \pm 5$  °C forming clear homogeneous mixtures. These were then gradually cooled (at a cooling rate of 2 °C per minute) at a thermostatic bath and the appearance of turbidity was taken to be the cloud point temperature.

### Calculation of viscosity through simulations

We consider a sample of polymer (melt or solution) placed between two parallel plates such that the adhesion between the sample and the plates is strong enough that there is no slippage at either surface. For simple shear along the  $x$ -direction, one may define the shear stress  $\sigma_{xy}$  as the ratio of applied force  $F$  and the cross sectional area  $A$  of the surfaces (which is also the area of any plane perpendicular to the  $y$ -direction within the material being sheared); that is,

$$\sigma_{xy} = \frac{F}{A} \quad (30.1)$$

The shear strain  $\gamma$  is defined as the displacement ( $\Delta x$ ) of the top plate relative to the thickness ( $h$ ) of the sample. Thus,

$$\gamma = \frac{\Delta x}{h} \quad (30.2)$$

For a perfectly elastic sample, the shear stress  $\sigma_{xy}$  and the shear strain  $\gamma$  are proportional and the constant of proportionality is known as the shear modulus  $G$ .

$$G = \frac{\sigma_{xy}}{\gamma} \quad (30.3)$$

Since the strain  $\gamma$  is dimensionless, the shear stress  $\sigma_{xy}$  and the shear modulus  $G$  have identical units of force/area. We now turn to impose a step strain of magnitude  $\gamma$  on the sample at time  $t = 0$ . For viscoelastic materials, the stress after such a step strain will have some general time dependence  $\sigma_{xy}(t)$ . The stress relaxation modulus  $G(t)$  is defined as the ratio of the stress remaining at time  $t$  (after a step strain was applied at time  $t = 0$ ) and the magnitude of this step strain  $\gamma$ :

$$G(t) = \frac{\sigma_{xy}(t)}{\gamma} \quad (30.4)$$

In order to obtain  $G(t)$  by simulation, one may consider a polymer chain of  $N$  beads which is subjected to a step shear deformation,  $\mathbf{E}$ , at time  $t = 0$ .

$$\mathbf{E} = \begin{pmatrix} 1 & \lambda & 0 \\ 0 & 1 & 0 \\ 0 & 0 & 1 \end{pmatrix} \quad (30.5)$$

Here,  $\lambda$  is a parameter characterizing the deformation. Following the application of the step deformation  $\mathbf{E}$ , the evolution of the bead positions may be calculated through the Langevin equation of motion (see later). The stress relaxation per segment of the chain is given by,

$$\sigma_{xy}(t) = \frac{1}{(N-1)} \sum_{i=1}^N F_{ix}(t) y_i(t) \quad (30.6)$$

where,  $F_{ix}$  is the  $x$ -component of the force on  $i$ th bead and  $y_i$  is the  $y$ -coordinate of its position vector  $\mathbf{r}_i$  ( $\equiv x_i, y_i, z_i$ ). All viscoelastic samples have a region of linear response at sufficiently small values of applied strain ( $\lambda \rightarrow 0$  in eq. (30.5)), where the relaxation modulus is independent of strain. Thus for the linear viscoelasticity of the sample, one may write the relaxation modulus as,

$$G(t) = \frac{1}{6(N-1)} \sum_{\alpha \neq \beta} \langle J_{\alpha\beta}(0) J_{\alpha\beta}(t) \rangle \quad (30.7)$$

with,  $J_{\alpha\beta}(t) = \sum_{i=1}^N F_{i\alpha}(t) \beta_i(t)$  and  $\alpha, \beta \equiv x, y, z$  ( $\alpha \neq \beta$  for calculating  $J_{\alpha\beta}$ ). The angular brackets signify the average over all the relaxation processes considered.

In the case of a binary blend system, a simple mixing rule for the stress relaxation function applies,

$$G(t) = \phi_1 G_1(t) + \phi_2 G_2(t) \quad (30.8)$$

where,  $\phi_1$  and  $\phi_2$  are the volume fractions of the components and the  $G_1(t)$  and  $G_2(t)$  are the corresponding shear relaxation moduli.

Finally, the viscosity  $\eta$  of any fluid is the time integral of its stress relaxation modulus,

$$\eta = \int_0^{\infty} G(t) dt \quad (30.9)$$

### Details of the Monte Carlo simulations

We employ a new model, Fraenkel + Lennard-Jones (LJ) for modeling both of the PEG and PEG-*ran*-PPG polymer chains. The polymer chains have been modeled as bead-spring chains of Lennard-Jones particles interacting through the Fraenkel potential (for the bead-bead backbone) and the repulsive Lennard-Jones potential (for the non-neighbor beads). The Fraenkel potential has a harmonic form

$$U_{\text{Fraenkel}}(r) = \frac{H_F}{2}(r - b_0)^2 \quad (30.10)$$

where,  $H_F$  is the force constant and  $b_0$  is the equilibrium bead-bead distance. The repulsive Lennard-Jones potential has been defined as

$$U_{\text{LJ}}(r) = 4\varepsilon \left[ \left( \frac{\sigma}{r} \right)^{12} - \left( \frac{\sigma}{r} \right)^6 \right] + \varepsilon, \quad r \leq (2)^{1/6} \sigma; \quad (30.11a)$$

$$U_{\text{LJ}}(r) = 0, \quad r > (2)^{1/6} \sigma; \quad (30.11b)$$

where,  $\sigma$  is the diameter of a bead and  $\varepsilon$  is the energy parameter representing the depth of the potential. This form of the LJ potential is also known as the Weeks-Chandler-Andersen (WCA) potential. The excluded volume effect of the polymer has been included in the repulsive LJ potential through the parameter  $\sigma$ . As the neighboring beads interact through the Fraenkel potential, the non-neighbor pairs interact through the repulsive LJ potential.

The PEG molecule is represented by a 20-beads Fraenkel + LJ chain [*i.e.*, 20 eg ( $\equiv$  ethylene glycol) repeat units] and the PEG-*ran*-PPG molecule is also modeled as a 20-beads Fraenkel + LJ chain comprising of 3eg-4pg-3eg-3eg-4pg-3eg repeat units (eg  $\equiv$  ethylene glycol and pg  $\equiv$  propylene glycol). For the PEG molecules, we have set  $H_F = 400 k_B T$ ,  $b_0 = 1.0 \sigma$  and  $\varepsilon = 0.83 k_B T$ ; where,  $k_B$  is the Boltzmann constant and  $T$  is the absolute temperature. These are in accordance with the simulation parameters for the Fraenkel + LJ chains of various lengths, as reported in the literature. In the PEG-*ran*-PPG molecules, we have repeating eg and pg units; for the eg units, we have kept the same energy and distance parameters (*viz.*,  $H_F = 400 k_B T$ ,  $b_0 = 1.0 \sigma$  and  $\varepsilon = 0.83 k_B T$ ), but for the pg units, the distance parameter is marginally incremented to  $b_0 = 1.01 \sigma$ , keeping the same energy parameter (*i.e.*,  $H_F = 400 k_B T$ ,  $b_0 = 1.01 \sigma$  and  $\varepsilon = 0.83 k_B T$ , for the pg units). The choice of the energy parameters has been kept the same as the bonding sequences of successive beads in eg, [-O-CH<sub>2</sub>-CH<sub>2</sub>-] and pg, [-O-CH(CH<sub>3</sub>)-CH<sub>2</sub>-] repeat units are more or less the same. In addition, the pg units have larger bead masses; as the masses of the eg and pg units are 44 g/mol and 58 g/mol respectively, the relative bead masses are in the ratio of 1:1.3182. For the interaction of hetero-bead pairs, the effective values of  $\sigma$  and  $\varepsilon$  are calculated from the Lorentz-Berthelot mixing rules.

$$\sigma_{ij} = \frac{1}{2}(\sigma_i + \sigma_j) \quad (30.12)$$

$$\varepsilon_{ij} = \sqrt{\varepsilon_i \varepsilon_j} \quad (30.13)$$

As the main interest of this chapter is to calculate the bulk properties, we have considered multiple chains for representing the pure components as well as the nine blends considered in this work. Table 30.1 gives the details of the systems simulated. During the Monte Carlo simulation of each of these systems, periodic boundary conditions have been applied, based on the position of the centre-of-mass of each chain.

**Table 30.1: Compositions of the systems simulated.**

PEG is poly(ethylene glycol), RAN is PEG-*ran*-PPG,  $\phi_i$  are the volume fractions,  $nchain_i$  are the number of 20-beads chains considered for the simulation,  $L$  is the edge length of the cubic simulation box.

System	$\phi_{PEG}$	$\phi_{RAN}$	$nchain_{PEG}$	$nchain_{RAN}$	$L / \sigma$
PEG	1.0	0.0	30	0	8.565
RAN	0.0	1.0	0	30	8.565
PEG10:RAN90	0.09	0.91	3	22	8.060
PEG20:RAN80	0.20	0.80	5	20	8.060
PEG30:RAN70	0.29	0.71	8	17	8.060
PEG40:RAN60	0.39	0.61	10	15	8.060
PEG50:RAN50	0.49	0.51	13	12	8.060
PEG60:RAN40	0.60	0.40	15	10	8.060
PEG70:RAN30	0.69	0.31	18	7	8.060
PEG80:RAN20	0.79	0.21	20	5	8.060
PEG90:RAN10	0.90	0.10	23	2	8.060

Initial configurations of chains of  $N$  beads have been generated as follows. Taking the first bead as the seed (placed arbitrarily at the origin), coordinates  $(x_i, y_i, z_i)$  of the successive beads are generated using  $(x_i = x_{i-1} + \sigma \sin \theta \cos \phi; y_i = y_{i-1} + \sigma \sin \theta \sin \phi; z_i = z_{i-1} + \sigma \cos \theta; \text{ for } i = 2, 3, \dots, N)$ ; angles  $\theta$  and  $\phi$  are obtained from  $\theta = \pi * qq$  and  $\phi = 2\pi * ff$  respectively, where  $qq$  and  $ff$  are two random numbers generated for each bead. Consecutive inter-bead distances are matched with  $\sigma$ , before accepting the coordinates of the new bead to build the chain. Once the first 20-beads chain has been made, its centre-of-mass (COM) is calculated and the chain is placed inside the cubic box. The second chain of the system was placed into the box in such a way that the COM of the second chain is at a radial distance of  $\sigma$ , from the COM of the first. The placement of the subsequent chains was done in a similar manner, avoiding overlap of the COMs. Each simulation box of a pure component (PEG or RAN) contains 30 chains, while the simulation box of a blend contains a total of 25 chains as given in Table 30.1. Each system was then equilibrated for  $10^6$  Monte Carlo (MC) steps during which several physical quantities were monitored. These include square of the end-to-end distance  $\langle R^2 \rangle$ , square of the radius of gyration  $\langle R_g^2 \rangle$  and square of the bond-segment distance  $\langle b^2 \rangle$  (see in Chapter 29, for details).

In the Langevin dynamics method, motion of each bead  $i$  of the chain is governed by a total force  $\mathbf{F}_i^T$  on the bead, which comprises of force arising from potential, frictional force and a random force.

$$\mathbf{F}_i^T = m \ddot{\mathbf{r}}_i = \mathbf{F}_i^C + \mathbf{F}_i^F + \mathbf{F}_i^R \quad (30.14)$$

where,  $m$  is the mass of the bead. The force arising from the chosen Fraenkel + LJ potential are included in  $\mathbf{F}_i^C$ . The frictional force acting on the bead is,  $\mathbf{F}_i^F = -\xi \mathbf{v}_i$ , where  $\mathbf{v}_i$  is the velocity of the bead and  $\xi$  is the friction coefficient. The friction coefficient  $\xi$  is related to the fluctuations of the random force  $\mathbf{F}_i^R$  through the fluctuation-dissipation theorem.

$$\langle \mathbf{F}_i^R(t) \rangle = 0 \quad (30.15a)$$

$$\langle \mathbf{F}_i^R(t) \cdot \mathbf{F}_j^R(t') \rangle = 6k_B T \xi \delta_{ij} \delta(t-t') \quad (30.15b)$$

The temperature  $T$  of the system being simulated is maintained through eq. (30.15).

In order to determine the dynamic viscosities, we have prepared the blend compositions by the melt mixing method at a fixed temperature of 150°C (see Section 30.3). Similarly, for the simulation purpose we choose a fixed temperature  $T = 1.2\varepsilon/k_B$ , defined by the LJ energy parameter,  $\varepsilon$  and the Boltzmann constant,  $k_B$ . This choice of temperature is identical with that used by other authors for the translocation studies on Fraenkel + LJ chains.

In the Monte Carlo simulation of the Langevin equation of a polymer chain, we replace the continuous time variable with a small time step  $\Delta t$ . If the position of the  $i$ th bead at time step  $t$  is denoted by  $\mathbf{r}_i(t)$ , the simulation form of the Langevin equation for the bead can be written as

$$\mathbf{r}_i(t + \Delta t) = \mathbf{r}_i(t) + \frac{d^2}{2k_B T} \mathbf{F}_i^T(t) + \mathbf{d}_i(t) \quad (30.16)$$

where,  $\mathbf{F}_i^T(t)$  is the total force on the  $i$ th bead at time  $t$ . The explicit form of the Langevin equation of motion in terms of friction coefficient ( $\xi$ ), bead mass ( $m_i$ ) and velocity relaxation time ( $\zeta^{-1}$ ) is given by

$$\mathbf{r}_i(t + \Delta t) = \mathbf{r}_i(t) + \frac{\Delta t}{\xi} \mathbf{F}_i^T(t) + \mathbf{d}_i(t) = \mathbf{r}_i(t) + \frac{\Delta t}{\zeta m_i} \mathbf{F}_i^T(t) + \mathbf{d}_i(t) \quad (30.17)$$

The random step vector  $\mathbf{d}_i(t)$  in eqs. (30.16) and (30.17) is characterized by the two moments,

$$\langle \mathbf{d}_i(t) \rangle = 0 \quad (30.18)$$

$$\langle \mathbf{d}_i(t) \mathbf{d}_j(t') \rangle = d^2 \mathbf{I} \delta_{ij} \delta(t-t') \quad (30.19)$$

where,  $\mathbf{I}$  is an unit tensor. The random displacement  $d$ , and time step  $\Delta t$ , are related through the diffusion constant  $D$ , of the chain.

$$d^2 = 2D\Delta t = \frac{2k_B T \Delta t}{\xi} \quad (30.20)$$

At the set temperature  $T$ , each of the simulation system was at first equilibrated for  $10^6$  Monte Carlo steps and to the resulting equilibrated configuration, step strain  $\mathbf{E}$  was applied at  $t = 0$

according to eq. (30.5), using  $\lambda = 0.5$  (for linear viscoelasticity). The small value of  $\lambda$  was chosen in order to ensure that the simulation  $G(t)$  is calculated in the linear region. We calculate the total force  $\mathbf{F}_i^T(t)$  on monomer  $i$  by eq. (30.14), followed by the position of the monomer in the next step  $\mathbf{r}_i(t + \Delta t)$  by eq. (30.16). Next, the stress tensor time correlation function  $G(t)$  is calculated using eqs. (30.7) and (30.8); finally, we integrate the  $G(t)$  to get viscosity  $\eta$  using eq. (30.9). Throughout this chapter, we report the simulation results using the following units: length in terms of  $\sigma$ , energy in terms of  $k_B T$ , force in terms of  $(k_B T / \sigma)$ , relaxation modulus as  $(k_B T / \sigma^3)$  and time as the Monte Carlo steps.

## Results

We have chosen a temperature of  $150^\circ\text{C}$  for the viscosity measurements in order to eliminate any crystallization possibility of the PEG component during the measurements. This was necessary as the cloud point measurements of all the samples showed the cloud point temperatures to have a maximum at ca.  $125^\circ\text{C}$ . The dynamic viscosities of the nine blend samples and also of the individual pure components (PEG and PEG-*ran*-PPG) were measured with the help of a Brookfield viscometer using the LV1 spindle at a speed of 0.3 rpm. The slowest speed of the spindle was chosen as the measurement of viscosities needed to be done with lowest measurable shear (so that the measurements are in the linear region). As usual, we took averages of three measurements and the scatter in the data is ca. 8 %. The dynamic viscosity values of the samples at  $150^\circ\text{C}$  have been shown as points in Figure 30.1. We have made an empirical fit of the relative viscosity of the PEG solutions as,

$$\frac{\eta}{\eta_{\text{PEG}}} = \exp(B\phi_{\text{PEG}}) \quad (30.21)$$

where,  $\eta_{\text{PEG}}$  and  $\phi_{\text{PEG}}$  are the viscosity and volume fraction of PEG, respectively. The fitting parameter  $B \approx 1.3$  gives the best fit of the viscosity data.

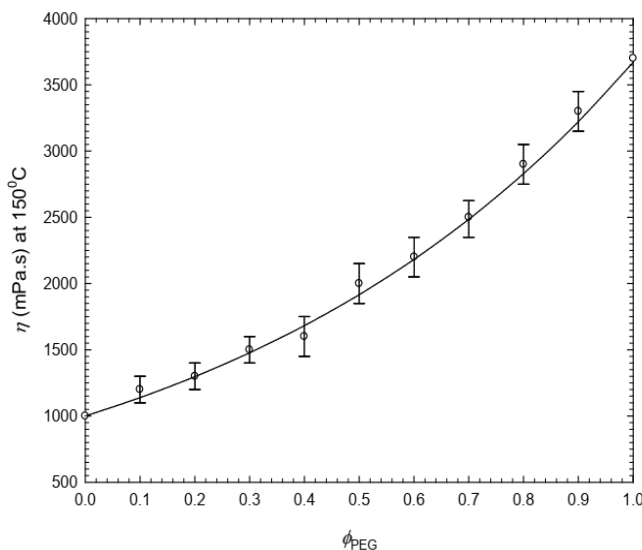
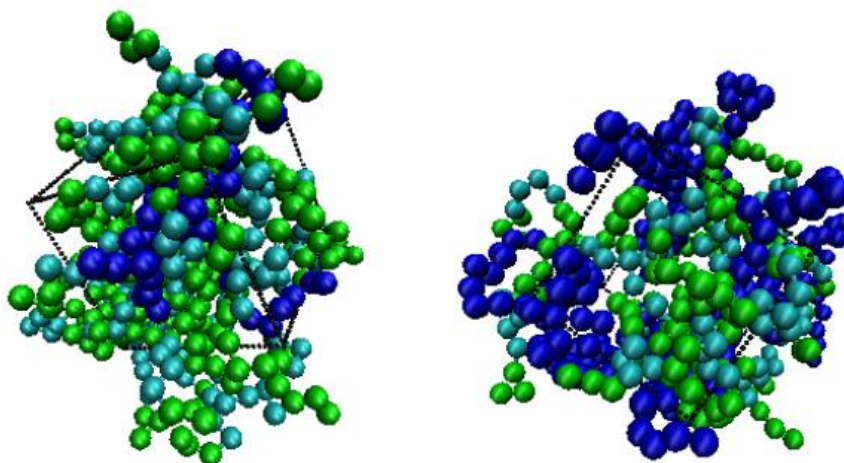


Figure 30.1: Experimental viscosities of the PEG, PEG-*ran*-PPG and the PEG:PEG-*ran*-PPG blends at  $150 \pm 5$  °C. Brookfield viscosities (model LVT, spindle LV1, speed 0.3 rpm) are shown as points; errors in the measurements ca.  $\pm 8$  %, as shown. The solid curve is an empirical fit of the data using the equation:  $\frac{\eta}{\eta_{\text{PEG}}} = \exp(B\phi_{\text{PEG}})$  where,  $\eta_{\text{PEG}}$  and  $\phi_{\text{PEG}}$  are the viscosity and volume fraction of PEG, respectively.  $B$  is a fitting parameter ( $\approx 1.3$ ).

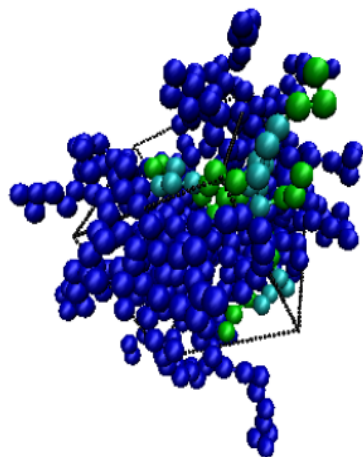
In order to supplement the dynamic viscosity data, coarse-grained Monte Carlo (MC) simulations were performed on each system. After the initial generation of the polymer chains (as detailed in Section 30.5), the equilibration of the 30 PEG chains (each of length  $N = 20$ ) and 30 PEG-*ran*-PPG chains (each of length  $N = 20$ ) had been done separately. In both the cases, the chains were subjected to the periodic boundary conditions applied on the basis of the coordinates of the centre-of-mass. This means, following the Langevin equation of motion [eq. (30.16)] of individual monomers, if the centre-of-mass of the chain moves out of the box, the chain needs to be brought inside the simulation box following the minimum image convention.

Figure 30.2 shows the snapshots of three typical blends with  $\phi_{\text{PEG}} \approx 0.1, 0.5$  and  $0.9$ . In the snapshots, the blue spheres represent eg monomers of PEG, the cyan or light blue spheres represent pg monomers of PEG-*ran*-PPG and the green spheres are representatives of eg monomers of PEG-*ran*-PPG (eg  $\equiv$  ethylene glycol, pg  $\equiv$  propylene glycol). The cubic simulation box with edges marked as black dots is also shown in each case. The snapshots are shown with a net packing fraction 0.5. As the periodic boundary conditions are applied on the centre-of-mass of the chains, a few monomers of both types of chains are seen to hang out of the edges of the cube.



(A) PEG10:RAN90 blend

(B) PEG50:RAN50 blend



(C) PEG90:RAN10 blend

Figure 30.2: Snapshots of three typical blend compositions with  $\phi_{\text{PEG}} \approx 0.1, 0.5$  and  $0.9$ . Color codes: blue: eg monomers of PEG, cyan: pg monomers of PEG-*ran*-PPG, green: eg monomers of PEG-*ran*-PPG (eg  $\equiv$  ethylene glycol, pg  $\equiv$  propylene glycol). The cubic simulation box (edges are marked as black dots) is also shown in each case. The snapshots are shown with a net packing fraction 0.5.

A typical relaxation modulus curve (*i.e.*, stress tensor time correlation function) has been shown in Figure 30.3, along with the empirical fits of the two groups of data points. The points in the figure are the simulated  $G(t)$  values for the PEG:PEG-*ran*-PPG::50:50 blend (v/v). It can be seen that the  $G(t)$  data exhibit a distinct bimodal characteristics. The ‘fast mode’ is the manifestation of the energetic-interactions-driven process which arises from the bond-segment-tension fluctuations. The later time ‘slow mode’ of the  $G(t)$  arises from the fluctuations in segmental

orientations and is driven by mainly entropic interactions. The fast mode (early time) can be described using a stretched exponential function,

$$G(t) = G(0) \exp\left(-\frac{t}{\tau}\right)^{\beta}, \quad 0 < \beta < 1 \quad (30.22)$$

where,  $\tau$  is the relaxation time of the fastest mode ( $\tau \approx 3.7$  MC steps, in this case) and the stretching exponent is  $\beta \approx 0.95 \pm 0.01$ . The fitting of the simulation data in the fast mode has been shown in Figure 30.3 as the red dashed curve. The slow mode (later time) exhibits a Rouse-like behavior and can be described using the mean field Rouse stress relaxation function,

$$G(t) = \frac{1}{(N-1)} \sum_{p=1}^{N-1} \exp\left(-\frac{t}{\tau_p}\right) \quad (30.23)$$

where,  $\tau_p$  is the relaxation time of the  $p$ th normal mode. The relaxation time,  $\tau_p$  is related to the friction coefficient  $\xi$ , the square of the bond-segment length  $\langle b^2 \rangle$  and the simulation temperature  $T$ ;  $k_B$  is the Boltzmann constant.

$$\tau_p = \frac{\xi \langle b^2 \rangle}{24k_B T \sin^2\left(\frac{p\pi}{2N}\right)} \quad (30.24)$$

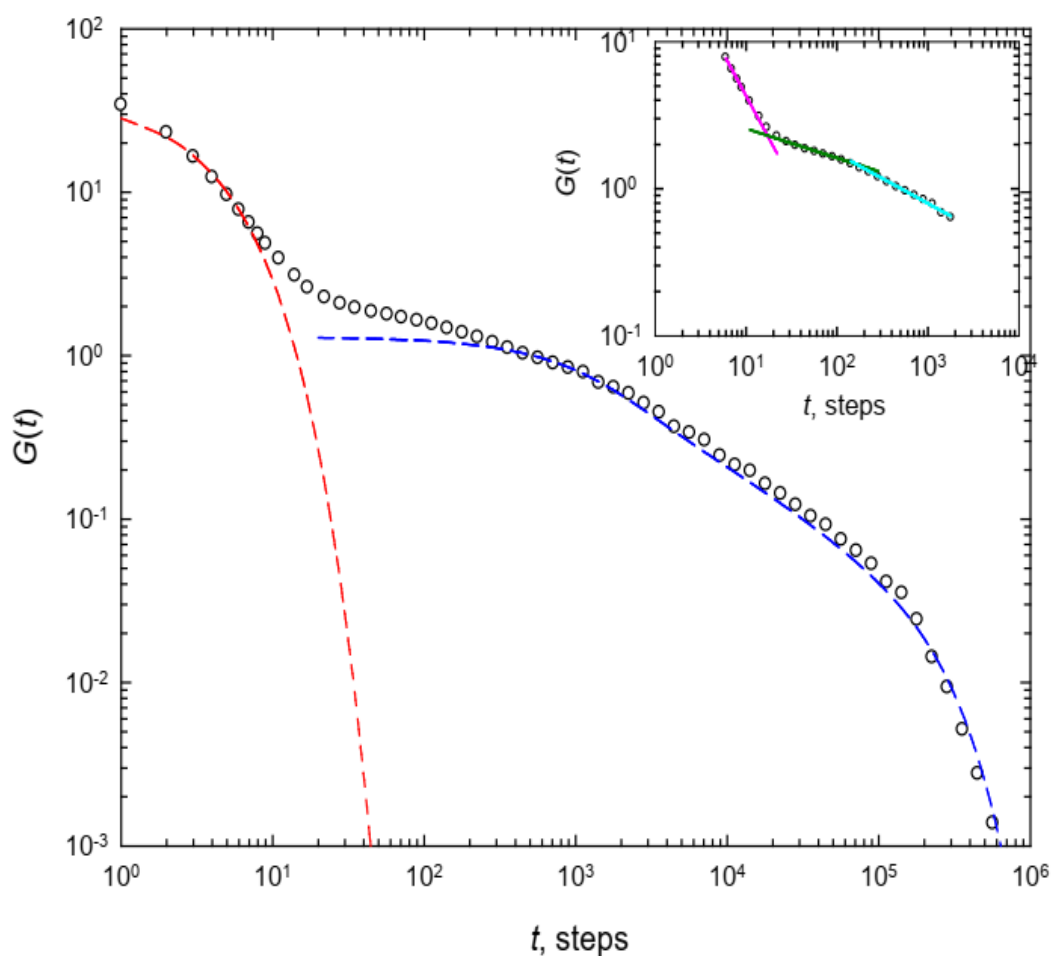


Figure 30.3: A typical relaxation modulus simulation curve for the PEG:PEG-*ran*-PPG blend (sample with  $\phi_{\text{PEG}} = 0.49$ ,  $\phi_{\text{RAN}} = 0.51$ ). Points are the  $G(t)$  values by simulation. The red dashed curve is the stretched exponential fit for the fast mode ( $\equiv$  energetic-interactions-driven mode) of  $G(t)$ . The blue dashed curve is the Rouse analytical fit for the slow mode ( $\equiv$  entropic-interactions-driven mode) of  $G(t)$ . The inset shows the fitting of the  $G(t)$  data for the ‘intermediate time region’ (i.e., from  $t \sim 5$  to  $t \sim 1000$  MC steps). The intermediate time region contains the ‘decay of the fast mode relaxation’ and the ‘onset of the slow mode relaxation’.

The slow mode simulation data in Figure 30.3 have been fitted to the Rouse analytical  $G(t)$  [eq. (30.23)] using the time shift factor 10.0 and the modulus shift factor 1.3. The fitting of the simulation data in the slow mode has been shown as the blue dashed curve in Figure 30.3.

We have also made empirical fits of the  $G(t)$  data in the ‘intermediate time region’ (*viz.* from  $t \sim 5$  to  $t \sim 1000$  MC steps). The fitting in this time region has been shown separately as the inset of Figure 30.3. The fitting equation is a power function in time given by,  $G(t) = Ct^{-\alpha}$ , where  $C$  and  $\alpha$  are fitting parameters. The intermediate time region accommodates the ‘decay of the fast mode (energetic-interactions-driven) relaxation’ and the ‘onset of the slow mode (entropic-interactions-driven) relaxation.’ The description of the dynamics of the chain in this time region is thus quite complex. For empirical fitting of the  $G(t)$  data, we found:  $C = 60.73$ ,  $\alpha = -1.15$ , for  $5 < t < 20$  (pink curve in the inset of Figure 30.3);  $C = 4.07$ ,  $\alpha = -0.20$ , for  $20 < t < 200$  (dark green curve in the inset);  $C = 8.31$ ,  $\alpha = -0.35$ , for  $200 < t < 1000$  (light blue curve in the inset). It would be exciting to work on the development of the physical insights corresponding to these time regions.

The fitting of the fast mode and slow mode  $G(t)$  data into respective analytical forms helps us to describe the time trace of the relaxation modulus in terms of well-known mathematical functions. In addition, we also get insights into the chain dynamics. Intuitively, in rheological measurements, the motion in the fast mode involves the application of shear and the immediate response of the sample to accommodate the applied shear (or applied step strain). The bond segments of the chain will attempt to relax the segment-tension due to applied shear (or due to applied step strain) through segment fluctuations and this happens within the first few moments. This is the origin of the fast mode. The segment-tension then spreads through the chain slowly and at a later time, the whole chain relaxes through randomization of its orientation, in the company of other chains, as friction becomes an important criterion. Hence the relaxation in this slow mode is entropic in nature. This slow relaxation of the chain can be conveniently described by the Rouse stress relaxation, where friction coefficient  $\xi$  and system temperature  $T$  have dominant influence on the chain behavior [see eqs. (30.23) and (30.24)]. It can be seen from Figure 30.3 that the  $G(t)$  data in the fast and slow modes contain an intermediate-time overlap region (described by the time of ca. 5 to 1000 MC steps) where the segment motions as well as overall chain motion are quite complex. As one of the major aim of the present article is to obtain viscosity data by simulation, we now proceed further to integrate the simulation  $G(t)$  data to obtain  $\eta$  through eq. (30.9).

We have generated the corresponding  $G(t)$  curves for pure PEG, pure PEG-*ran*-PPG and the nine blend compositions. For the nine blend compositions,  $G(t)$  data have been obtained through eq.

(30.8), using the calculated component volume fractions,  $\phi_i$  and the component  $G_i(t)$ s. In each case we have taken averages of 20 runs (with different initial configurations) and the errors in measurement are about  $\pm 1\%$ . These averaged  $G(t)$  curves were then integrated to obtain  $\eta^{\text{simul}}$  using eq. (30.9). Figure 30.4 presents the simulated viscosity data of the pure and the blend systems. The points in Figure 30.4 can be fitted to an empirical equation:  $\frac{\eta^{\text{simul}}}{\eta_{\text{PEG}}^{\text{simul}}} = \exp(K\phi_{\text{PEG}})$  where,  $\eta_{\text{PEG}}^{\text{simul}}$  and  $\phi_{\text{PEG}}$  are the simulation viscosity and volume fraction of PEG, respectively;  $K$  is a fitting parameter ( $\approx 1.05 \pm 0.02$ ).

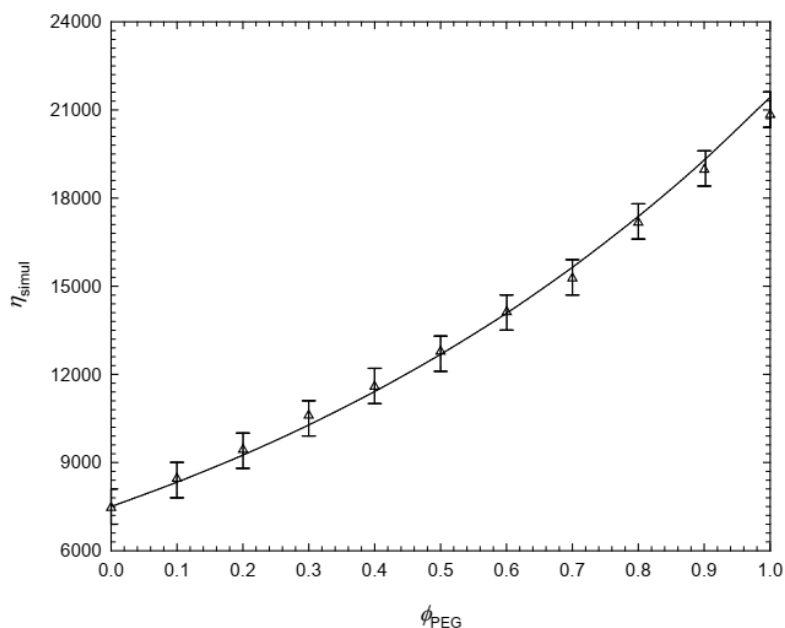


Figure 30.4: Viscosities by simulation at  $k_{\text{B}}T/\varepsilon = 1.2$ , of the PEG, PEG-*ran*-PPG and the PEG:PEG-*ran*-PPG blends. The points are the averages of 20 runs with errors ca.  $\pm 1\%$ , as shown. The solid curve is an empirical fit of the data using the equation:  $\frac{\eta^{\text{simul}}}{\eta_{\text{PEG}}^{\text{simul}}} = \exp(K\phi_{\text{PEG}})$  where,  $\eta_{\text{PEG}}^{\text{simul}}$  and  $\phi_{\text{PEG}}$  are the simulation viscosity and volume fraction of PEG, respectively.  $K$  is a fitting parameter ( $\approx 1.05$ ).

### Matching of the experimental data and the simulation data

It is interesting to note that the empirical equation fitting the simulation viscosity data is in principle similar to the equation which fitted the experimental Brookfield viscosities at  $150^{\circ}\text{C}$  of the blends. Therefore, we combine the two sets of  $(\phi_{\text{PEG}} - \eta)$  data into a single plot and this has been shown in Figure 30.5. The red dots are the Brookfield viscosities measured at  $150^{\circ}\text{C}$  while the blue triangles are the simulated viscosities at a temperature  $k_{\text{B}}T/\varepsilon = 1.2$ . The red and blue

colored arrows in the figure point to the respective ordinates of the plots. The reasonably good match of the experimental and simulated viscosities in Figure 30.5 emphasizes the validity of the model chosen for simulation as well as the reliability of the Brookfield viscosity data measured at 150°C.

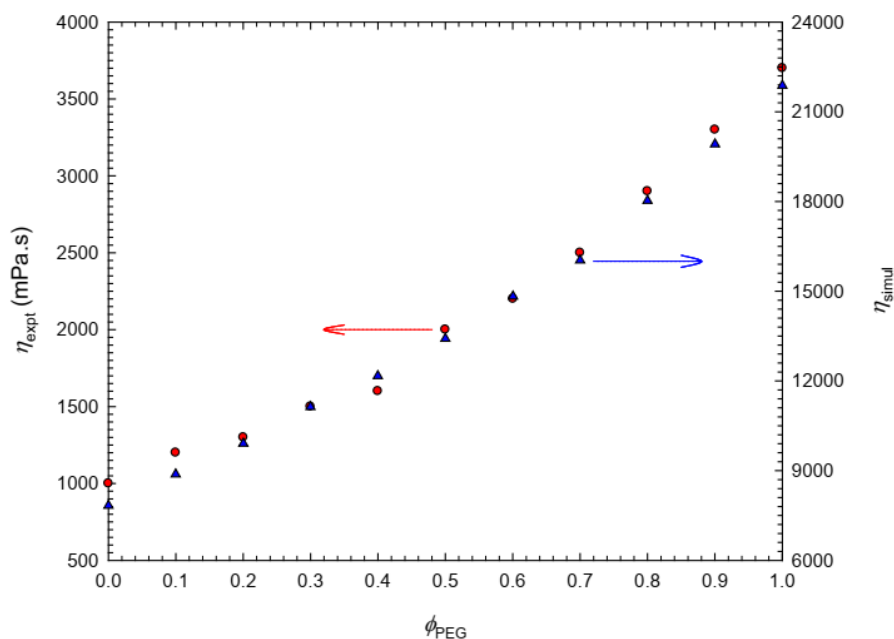


Figure 30.5: **Experiment vs simulation.** Brookfield viscosities (red points) of the PEG, PEG-*ran*-PPG and the PEG:PEG-*ran*-PPG blends at  $150 \pm 5$  °C are compared with the viscosities by simulation (blue triangles) at  $k_{\text{B}}T / \varepsilon = 1.2$ . The colored arrows point to the ordinates of the respective data points.

## Recommendations

1. Learn about the Rouse model from a text book on Polymer Physics.  
M. Rubinstein, R. H. Colby, *Polymer Physics*, Oxford University Press, Oxford, 2003.
2. Learn about the miscibility of the two polymeric substances discussed in this chapter.  
A. K. Das, D. Y. Hsu, P. D. Hong; *Macromolecular Theory and Simulations*, **2011**, 20, 19-30.

## Questions

1. What are the reasons for choosing a speed of 0.3 rpm of the spindle in the measurements of viscosities?

2. Why the WCA potential was chosen in addition to the Fraenkel potential?
3. The simulation temperature was set to be,  $T = 1.2\varepsilon/k_B$ . Why the temperature needs to be defined in terms of the Lennard-Jones parameter  $\varepsilon$ ?
4. What is the origin of the fast mode of stress relaxation?
5. What is the origin of the entropic mode of stress relaxation?